Direct Wind Accretion and Jet Launch in Binary Systems

Maxim V. Barkov[1,2], Dmitry V. Khangulyan[3]

[1]*Max-Planck-Institut für Kernphysik, Saupfercheckweg 1, 69117 Heidelberg, Germany*
[2] *Space Research Institute, 84/32 Profsoyuznaya Street, Moscow 117997, Russia*
[3] *Institute of Space and Astronautical Science/JAXA, 3-1-1 Yoshinodai, Chuo-ku, Sagamihara, Kanagawa 252-5210, JAPAN*

ABSTRACT
In this paper we study the wind accretion onto a rotating black hole in the close binary system harboring a young massive star. It is shown that the angular momentum of the accreted stellar wind material is not sufficient for the formation of an accretion disk. On the other hand, in the considered conditions the Blanford-Znajek mechanism can be activated, thus powerful jets can be launched in the direction of the rotation axis of the black hole. Importantly, no observational signatures of accretion, as typically seen from the thermal X-ray emission from the accretion disks, are expected in the suggested scenario. Here, properties of the generated jet are studied numerically in the framework of a 2D general relativity magnetohydrodynamical approach. Due to the accumulation of the magnetic flux at the black hole horizon, the jet power is expected to be modulated on a sub-second time-scale. Although the intervals between jet active phases depend on the magnetic flux escape from the black hole horizon (which can be modeled self-consistently only using a 3D code), a general estimate of the averaged jet power is obtained. It is expected that for the black hole rotation, expected in stellar binary system (the dimensionless rotation parameter $a = 0.5$), approximately 10% of the accreted rest energy can be channeled into the jets. In the specific case of the gamma-ray binary system LS 5039, the obtained jet luminosity can be responsible for the observed GeV radiation if one invokes Doppler boosting, which can enhanced the apparent flux from the system.

Key words: gamma-rays: stars, stars: individual: LS 5039, jets, binaries, accretion

1 INTRODUCTION

Several binary systems, consisting of a massive star and a compact object (CO) –neutron star (NS) or black hole (BH)– were detected in the very high energy (VHE) regime (Aharonian et al. 2005b,a, 2006, 2009; Albert et al. 2006, 2007, 2009; Acciari et al. 2008, 2009, 2011), and their non-thermal emission is believed to be linked to the processes related to the CO (see e.g. Bosch-Ramon & Khangulyan 2009, for a review). Moreover, given large values of gamma-gamma opacity expected in the close vicinity of CO, the VHE gamma-ray production most likely should be related in the outflow originated in the CO. In particular, in the system PSR B1259−63/LS2883 a pulsar is orbiting a massive O-type star (see Negueruela et al. 2011, and reference therein), and the detected X-ray and TeV radiation is attributed to synchrotron and inverse Compton (IC) emission produced by electrons accelerated at the pulsar wind termination shock (Kirk et al. 2000; Khangulyan et al. 2007; Uchiyama et al. 2009), while emission detected in the GeV energy range (Tam et al. 2011; Abdo et al. 2011) can be explained by the bulk Comptonizaiton of the pulsar wind (Khangulyan et al. 2011). In the case of Cygnus X-1, the evidence of detection in TeV found MAGIC (Albert et al. 2007) is most likely related to the non-thermal activity occurring in the jet launched by a black hole (Esin et al. 1998) accreting matter from a O9.7Iab star (Ziółkowski 2005).

The classification of compact objects (CO) in these two cases

is rather clear since (i) pulsed radio emission coherent with the orbital motion is detected from PSR B1259−63/LS2883 (Johnston et al. 1996); and (ii) in the case of Cygnus X-1 the mass of the CO exceeds the Oppenheimer-Volkoff upper limit for the mass of NS (Casares 2007), and the accretion disk is clearly seen in the X-ray energy band (Esin et al. 1998).

The physical processes responsible for the VHE radiation detected from two other systems, LS 5039 and LS I +63−303, is still debated, since currently there is no observational evidences which allows robust conclusions regarding the nature of the CO. In particular, despite intensive searches no pulsed emission has been detected from these systems. Although, strong free-free absorption, expected in these relatively compact binaries, could hide the radio pulsations (Dubus 2006), the strict upper limits obtained in the X-ray energy band (Rea et al. 2010, 2011) pose additional constraints for the realization of the binary pulsar scenario in these systems. Another, independent on the orientation of the "pulsar beam", another test for the presence of a pulsar in the binary system is related to the impact of the pulsar wind on the stellar environment. Namely, the collision of the stellar and relativistic pulsar winds should give rise not only to the non-thermal emission related to the pulsar wind, but the stellar wind would be also shocked producing thermal X-rays. This approach was used to constrain the spin-down (SD) luminosity of the possible pulsar in the case of LS 5039 (Zabalza et al. 2011). Importantly, the derived upper lim-

its appeared to be very close to the non-thermal luminosity detected with *Fermi* Large Area Telescope (*Fermi*/LAT) (Abdo et al. 2009a). Thus, one should expect either a perfect conversion of the pulsar energy to GeV gamma-ray, or to invoke Doppler boosting of the emission. Although, the relativistic motion of the shocked pulsar wind is a rather natural effect in binary pulsar systems (Bogovalov et al. 2008; Khangulyan et al. 2008; Dubus et al. 2010), fast mixing of the stellar and pulsar winds may destroy the relativistic regime of the outflow (Bosch-Ramon & Barkov 2011), and the efficient Doppler boosting of the emission is possible only on the scales limited by the binary system size.

Orbital phase dependent extended radio structures, predicted for the binary pulsar systems Dubus (2006), were found in the gamma-ray binary systems PSR B1259−63/LS2883, LS 5039 and LS I +63−303 (Dhawan et al. 2006; Ribó et al. 2008; Moldón et al. 2011a,b). This may be considered as a strong evidence for the presence of pulsars in these systems, however (i) the extended radio emission can be naturally produced in gamma-ray binary systems via the synchrotron emission of secondary pairs (Bosch-Ramon et al. 2008; Bosch-Ramon & Khangulyan 2011); (ii) to interpret the resolved structures requires a knowledge of the flow dynamics that presently lacks. This uncertainty can be to some extend explained by the excessive simplification adopted in the theoretical calculations, in particular the interaction of the winds in binary pulsar can be rather complicated (Bogovalov et al. 2008; Bosch-Ramon & Barkov 2011) and differ significantly (Bogovalov et al. 2011) from the case realized at the interaction of a pulsar with the interstellar medium (Kennel & Coroniti 1984; Dubus 2006). Thus, the interpretation of these observations in the context of the pulsar scenario remains inconclusive.

An alternative scenario implies the production of VHE gamma-rays in miroquasar jets launched by an accreting black hole. Although both systems, LS 5039 and LS I +63−303, do not show thermal emission produced by the accreation disk, as it is expected in the classical microquasar (*μ*Q) paradigm, the spectroscopic observations of LS 5039 favor a mass of the CO (Casares et al. 2005; Sarty et al. 2011) exceeding the Oppenheimer-Volkoff upper limit for the mass of NS. If a BH is indeed located in these systems, the absence of the thermal emission of the accretion disk might be interpreted as a signature of the *radiatively non-efficient* disk accretion (Narayan & Yi 1994; Blandford & Begelman 1999), although the applicability of these scenarios is debated for sub-Eddington stellar systems (Artemova et al. 2006). Therefore, a detailed study of the properties of the accretion flow in binary system is required for meaningful conclusions regarding the possibility to power these sources, LS 5039 and LS I +63−303, by accretion. We show below that in these systems of massive stars, which do not fill the Roshe lobe and the CO is not very massive, the accretion onto the BH should occur from the stellar wind.

For the sake of specificity, we adopt in this work the system parameters similar to those of LS 5039. In this system the CO is orbiting an O6.5V star in a relatively non-eccentric orbit (see the system parameters in Tab. 1). This system was detected as a bright non-thermal source in a very broad energy range, from radio to VHE (see e.g. Bosch-Ramon & Khangulyan 2009, and references therein). The spectral energy distribution (SED) of the radiation is dominated by GeV gamma-rays. Namely, a flux of about few×10^{35} erg cm^{-2}s^{-1} was detected with *Fermi*/LAT (Abdo et al. 2009b). The fluxes in X-ray and TeV energy bands are comparable and at the level of ∼ 10^{34} erg cm^{-2}s^{-1} (Aharonian et al. 2006; Takahashi et al. 2009). X-ray, GeV and TeV emission components were shown to be periodic and stable on year time-scales (Aharo-

nian et al. 2006; Kishishita et al. 2009; Abdo et al. 2009b). We note that the emission detected from LS I +63−303 is known to differ significantly from orbit to orbit (Li et al. 2011; Acciari et al. 2011).

According to our analytical estimates, the accretion rate can be relatively high, in agreement with the results obtained by Owocki et al. (2011). Importantly, due to the lack of angular momentum, the accretion proceeds without the formation of an accretion disk, i.e. one should not expect detectable thermal X-rays from the infalling matter. Despite the absence of the accretion disk, our study shows that a powerful jet can be launched in this accretion regime. The crucial conditions for the formation of a powerful jet are (i) magnetization of the in-falling flow; and (ii) high enough accretion rate. If these conditions are fulfilled, a fast rotating BH can power and launch a magnetically driven jet (Komissarov & Barkov 2009). Accretion of the matter leads to the accumulation of the magnetic flux near the BH. When the B-field reaches the critical value, the magnetic pressure pushes out the in-falling matter pausing the accretion and dis-power the jet. This phenomenon is similar to the well known *magnetically arrested disks* (Bisnovatyi-Kogan & Ruzmaikin 1974, 1976; Kaisig et al. 1992; Narayan et al. 2003; Igumenshchev 2008; Romanova et al. 2009; Tchekhovskoy et al. 2011). The periodic stops of the central engine leads to a formation of a quasi-periodic structure of the jet on a scale significantly smaller (by three orders of magnitude) than the system semi-major axis.

The paper is organized as following: in Sect.2 we present the general properties of the accretion flow in binary systems; in Sect. 2.2 we develop a 2D general relativity magnetohydrodynamical (GRMHD) numerical model for the accretion flow, and study different accretion regimes; in Sect. 3 we discuss the implications of the obtained solutions; and in Sect. 4 we summarized the obtained results.

2   MODELING ACCRETION

2.1   General Properties of the Accretion Flow

In a binary system harboring the BH, and in which the optical component does not fill the Roshe lobe, the BH will accrete from the stellar wind directly. The accretion rate can be estimated from the Bondi-Hoyle solution, which describes the accretion onto a center of mass M moving with a constant speed v_∞ through a uniform medium of density ρ_∞. The Bondi-Hoyle mass accretion rate is well approximated by the equation

$$\dot{M}_{BH} = \pi R_A^2 \rho_\infty v_\infty \,, \tag{1}$$

where

$$R_A = \frac{2GM}{v_\infty^2} \tag{2}$$

is the accretion radius. In the Bondi-Hoyle solution the mean angular momentum of accreted matter is zero.

The wind accretion can be only marginally described by the Bondi-Hoyle solution due to the density and velocity gradients across the BH trajectory, although provided that the gradients are small on the scale of the accretion radius, the above expression for $\dot{M}$ is still quite accurate (Ishii et al. 1993; Ruffert 1997, 1999). However, the accreted matter can obtain a non-zero mean angular momentum (Illarionov & Sunyaev 1975; Ishii et al. 1993; Davies & Pringle 1980; Ruffert 1997, 1999). In analogy to the work by Barkov & Komissarov (2011) given the unsettled nature of this is-

Table 1. The parameters of the system LS5039

Description	Designation	Value
Mass of star	M_s	$26 M_\odot$
Radius of star	R_s	$9.3 R_\odot$
Temperature of the star	T_s	$39,000$ K
Stellar Wind termination velocity	V_∞	$2,400$ km/s
Stellar Wind loss rate	$\dot{M}_s$	$4 \times 10^{-7} M_\odot \mathrm{yr}^{-1}$
Orbital period	P_s	3.9 day
Eccentricity of the orbit	e	0.24
The mass of the BH	M_{BH}	$3 M_\odot$
Semimajor axis	a_o	$3.5 R_s$

sue, we will assume that the mean specific angular momentum of accreted matter inside the accretion cylinder is

$$\langle j_A \rangle = \frac{\eta}{4} \Omega R_A^2, \tag{3}$$

where Ω is the angular velocity of the orbital motion; and η is a free parameter ($|\eta| < 1$), which reflects our current ignorance.

In the specific case of LS 5039, the above estimates allow us to obtain analytically approximate values for the accretion rate and angular momentum of the flow. The physical properties of the system are summarized in Table.1 (see Casares et al. 2005; Sarty et al. 2011, and the references therein).

The wind velocity profile can be approximated as (Kudritzki & Puls 2000)

$$v_w(R) \approx v_\infty \left(1 - \frac{R_s}{R}\right). \tag{4}$$

Thus, the typical wind velocity at the orbital separation distance, a_o, can be estimates as $v_w(a_o) \approx 1.7 \times 10^8$ cm s^{-1} (see Table. 1, for the used parameter values). This value exceeds significantly the orbital velocity of the BH, $v_o \approx 4 \times 10^7$ cm s^{-1}, thus in the calculation one can safely neglect the BH velocity. Substituting the wind speed to Eq.(1) one obtains the value for the BH accretion rate:

$$\dot{M}_{BH} = 1.5 \times 10^{-11} M_\odot \mathrm{yr}^{-1}. \tag{5}$$

We note that this value depends on the star separation distance and can vary up to a factor of 3-5 along the orbit (Owocki et al. 2011). Note, that the accretion rate in the system LS 5039 is significantly smaller than in the case of Cygnus X−1 due to large difference in the masses of CO and in the speed of the stellar wind.

Follow Eq.(2), which gets $R_A \approx 2.7 \times 10^{10}$ cm, after it substitution in Eq.(3) one can obtain the value for the angular momentum of the accreted matter $j_A = 3.3 \times 10^{15}$ cm^2 s^{-1}. This value appears to be small as compared to the specific angular momentum related to the last marginally bound orbit, $j_{mb} \approx 3.4 r_g c = 3.4 G M_{BH}/c \approx 4.5 \times 10^{16}$ cm^2 s^{-1} (here we assume the BH dimensionless rotation parameter to be $a = 0.5$) (Bardeen et al. 1972). This relation, $j_A \ll j_{mb}$, implies that the accretion disk cannot be formed in such an accretion regime, and one should expect a nearly spherically symmetric in-flow of the stellar material. This allows to perform the calculations of the accretion under 2D approximation. Namely, we study the case of the spherical accretion onto a rotating black hole (the setup is similar to ones considered by Komissarov & Barkov 2009; Barkov & Komissarov 2010). The initial magnetic field is assumed to be homogeneous on the scale of the computational domain $R_{com} = 2 \times 10^9$ cm, and parallel to the rotation axis of BH. The accretion rate was assumed to be steady on the computational time-scale, and two values were adopted $\dot{M}_{BH} = (1.5 \text{ and } 8) \times 10^{-11} M_\odot \mathrm{yr}^{-1}$.

2.2 Numerical results

The main details of our numerical method and various test simulations are described in the literature (see for details Komissarov 1999, 2004, 2006; Komissarov & Barkov 2007). Here we outline just the key elements of the approach. The calculations are performed in Kerr-Schild spacetime coordinates. The computational grid was selected to be uniform in polar angle, θ, where it has 320 cells and logarithmic in spherical radius, r, where it has 773 cells. The inner boundary is located just inside the event horizon and adopts the free-flow boundary conditions. The outer boundary is located at $r = 2.2 \times 10^9$ cm and at this boundary the flow is prescribed according to the free-fall Bondi model with constant accretion rate.

In our study we check the feasibility the Blanford-Znajek (BZ) driven jet formation (Ruffini & Wilson 1975; Lovelace 1976; Blandford & Znajek 1977) in the specific conditions of wind accretion in the gamma-ray binary system LS 5039. Simple relations obtained by Barkov & Komissarov (2008b) relate the BZ energy realize to the magnetic flux

$$L_{BZ} = 1.4 \times 10^{35} f(a) \Psi_{20}^2 \left(\frac{M_{BH}}{10 M_\odot}\right)^{-2} \mathrm{erg\ s}^{-1}, \tag{6}$$

where $f(a) = a^2 \left(1 + \sqrt{1 - a^2}\right)^{-2}$ is a dimensionless function accounting for the BH rotation; and $\Psi_{20} = \Psi/10^{20}$ G cm^2 is the magnetic flux. According to Barkov & Komissarov (2010), the expected value of the dimensionless rotation parameter of the BH in a stellar binary system should be relatively small, namely $a = 0.5$ ($f(a) = 0.072$).

Regarding the strength of the initial magnetic field, to reduce the calculation time we have assumed a fixed value of 10^3 G, which exceeds significantly the value of a few G expected in stellar binary systems. We note that the actual value of the magnetic field strength affects only the duration of the magnetic flux accumulation stage, but does not influence the energy release at the saturation phase (see details below). Thus, the assumption of a strong magnetic field does not influence our results while allowing to reduce significantly the computation time.

At the initial stage of the simulation spherically symmetric accretion occurs and the magnetic flux accumulates on the horizon of the BH. At the moment when the magnetic flux exceeds the critical value (see Barkov & Komissarov 2008a; Komissarov & Barkov 2009, for more details), the BZ mechanism gets activated and a magnetically driven jet is launched. The accumulation phase can be clearly seen in Fig. 1, as the lower trajectory in the *magnetic flux vs square root of the jet power* phase space. Namely, during this period the system is characterized by an increasing magnetic flux without any ejection of energy. This is caused a too low value of the magnetic torque to activate the BZ mechanism.

The flux accumulation stage (marked with number 1 in Fig.1) continues until the magnetic field flux reaches the critical value of $\Psi \approx 10^{20}$ G cm^2 for an accretion rate of $\dot{M}_{BH} = 8 \times 10^{-11} M_\odot \mathrm{yr}^{-1}$ (see transition in Fig.1, left panel). This value of magnetic flux can be used to check the feasibility of the jet activation in binary systems with relatively weak magnetic field (we remind that in the calculations we have assume a large value of B-field for the sake of reducing of the computational expenses). The required value can be reached even in the case of accretion of an uniform magnetic field of strength $B_w \sim 0.1 \dot{M}_{-10}^{1/2}$ G from the radius $R_A \simeq 3 \times 10^{10}$ cm. We note that stellar winds can carry significantly stronger magnetic fields (see eq. Usov & Melrose 1992).

Once the jet is launched, the dense falling plasma is evacu-

ated from the BH magnetosphere, and the BZ mechanism starts to operate in the conventional way. Thus, the jet power should be described by Eq. (6). Indeed, in Fig. 1 one can see that after the accumulation/cleaning (marked with numbers 1 and 2 in the figure) stages the system remains on a straight line $L_{BZ}^{1/2} \propto \Psi$ (marked with number 3 in the figure).

The jets are ejected in the directions of the BH rotation axis and blow up bubbles, as it is shown in Fig.2 (right top panel). In the zoomed image of the central part, shown in Fig.2 (left top panel), one can see that the matter in-falling occurs through a narrow region in the equatorial plane. However we note, that although this can mimic a thin accretion disk (Bisnovatyi-Kogan & Ruzmaikin 1974, 1976), the matter velocity has no rotational component in this region. This can be clearly seen from the left bottom panel in Fig.2, where the ratio of toroidal and poloidal components of the B-field are shown. Any toroidal velocity component would lead to an enhancement of the corresponding (i.e. toroidal) magnetic field component. It is noteworthy that this configuration with radial accretion along the equatorial plane does not significantly differ from the standard disk accretion (which was adopted in the conventional BZ mechanism) in the regions close to the BH horizon since, even in the case of disk accretion, a free falling region is formed inside the marginally stable orbit.

Another important aspect of the considered accretion regime is shown in Fig.2 bottom right panel, where the ratio of gas and magnetic pressures is shown. It can be seen that in the equatorial region the gas pressure dominates, but the jet itself is strongly dominated by the magnetic pressure. This configuration fits perfectly the paradigm of the magnetically driven jets, where the gas pressure in the jet is expected to be negligible, while in the equatorial plane the presence of matter is required to keep a strong magnetic field near the horizon.

The time dependence of the jet power is shown in Fig.3. It can be seen that after the magnetic flux accumulation stage, the jet power starts to increase quickly. This growing phase is stopped by a sudden drop of the jet power. This is caused by gradual increase of the magnetic field flux at the BH horizon during accretion. When the magnetic pressure overtakes the in-falling matter ram pressure, a fast change of the structure of the B-field occurs, leading to the formation of a *magnetically arrested torus*, as shown in Fig.4. A similar situation is discussed by Narayan et al. (2003); Igumenshchev (2008) for the case of disk accretion.

Since in the case of a *magnetically arrested torus* no accretion occurs, a fast increase of the gas pressure is unavoidable. Once the gas pressure reaches a value exceeding the B-field pressure, the accretion, as well as the jet power supply, are resumed. We note however that in the case of a 3D setup a natural escape of the magnetic flux can be realized through the generation of *magnetic tubes*. In principle, this could lead to the formation of a nearly steady flow, although a quasi periodic pattern may still remain in the jet power time dependence. A detailed study of this issue is beyond the scope of this paper and will be discussed elsewhere, below we present a qualitative discussion of this effect, which despite of qualitative still allows rather fundamental conclusions. In the frameworks of 2D calculations, a quasi periodic consequence of "on/off" phases is expected. For the computational B-field strength the typical period of these oscillations is a fraction of a second. In fact for a large range of the wind magnetic field value, this period depends only on the accretion rate and BH mass (see for detail Sect. 3).
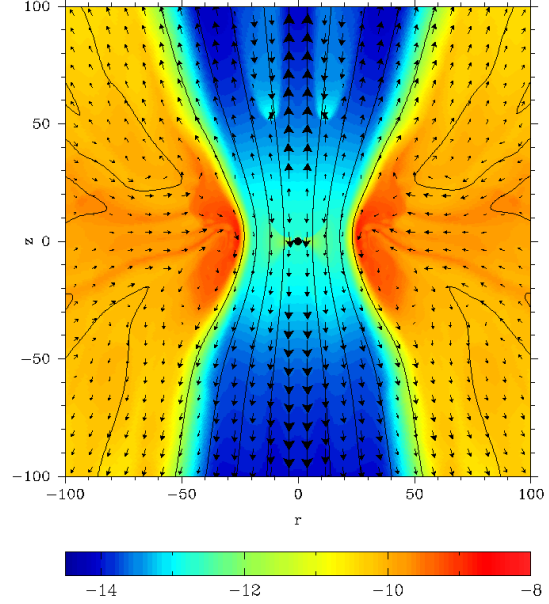
Figure 4. The flow configuration corresponding to the "magnetically arrested" regime. The solid lines show the magnetic field lines and the arrows indicate the flow velocity (both the direction and the absolute value). The color corresponds to $\log \rho$. It can be seen that the accretion is stopped at this moment and jet ejection is significantly less efficient as compared to the configuration shown in Fig. 2. The initial magnetic field in the stellar wind was assumed to be 10^3 G, and the accretion rate was selected to be $\dot{M}_{BH} = 8 \times 10^{-11} M_\odot \text{yr}^{-1}$. The shown snapshot of the flow corresponds to the time moment $t = 0.159$ s after the accretion was initiated (this moment corresponds to the "paused jet" as seen in Fig. 3).

3   DISCUSSION

The obtained numerical solution may have some interesting implications for the phenomenological study of μQs. Namely, it was shown that an effective jet launch is possible in binary systems in the case of the direct wind accretion, i.e. without the formation of an accretion disk. Since the present phenomenological description of the processes occurring in μQs relays on the observational appearance of the accretion disk, which lacks in the case of direct wind accretion μQs should fall out from this framework. Although the in-falling matter gets strongly heated at the termination shock of the in-falling matter, given the very short free-fall and dynamical time-scales compared to the cooling time, no detectable thermal emission is produced in the framework of the scenario. Thus, the only way to obtain observable features of the suggested scenario is to study in detail the properties of the jet, and in particular its modulation properties.

3.1   Jet internal time-scales

As it was discussed above the reason behind the strong modulation ("on/off" states) of the jet power is the accumulation of the magnetic field flux at the BH horizon. When the magnetic field pressure exceeds the ram pressure of the accretion flow, accretion is stopped and the jet switches off. It is possible to estimate the variability time from the comparison of the two key forces: magnetic pressure

$$P_m = \frac{B^2}{8\pi} = \frac{\Psi^2}{8\pi^3 R^4} , \qquad (7)$$
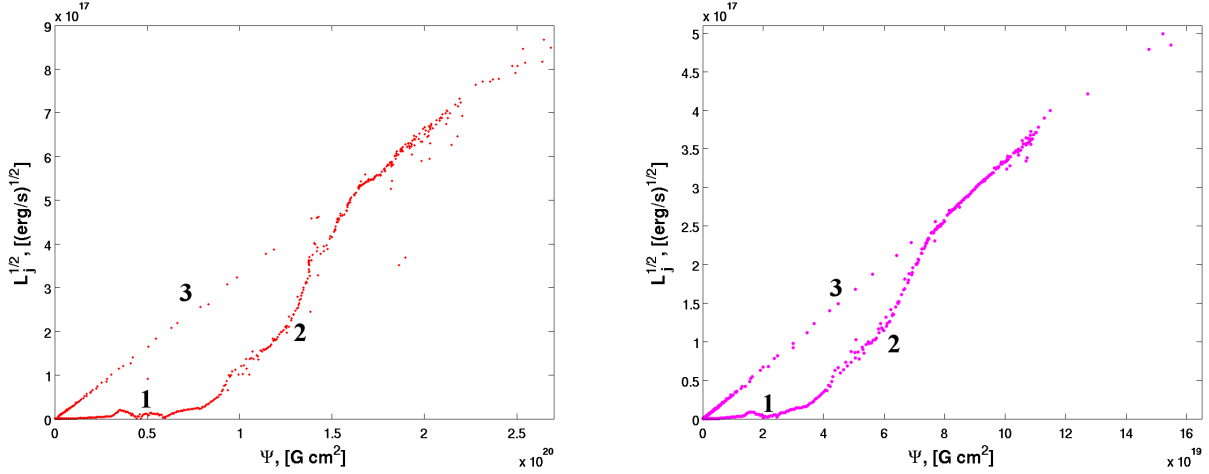
Figure 1. The square root of the jet luminosity as a function of the magnetic flux, Ψ, accumulated at the BH horizon. Three different regimes can be seen in the figure: (i) the initial accumulation of the magnetic flux (marked with "1"); (ii) transition to the BZ regime (marked with "2"); and (iii) the conventional BZ regime, when a linear dependence $L_j^{1/2} \propto \Psi$ is expected (marked with "3"). The initial magnetic field in the stellar wind was assumed to be 10^3 G, and two accretion rates were considered $\dot{M}_{BH} = 8 \times 10^{-11} M_\odot \mathrm{yr}^{-1}$ (left panel); and $\dot{M}_{BH} = 1.5 \times 10^{-11} M_\odot \mathrm{yr}^{-1}$ (right panel).

and gravitational hydrostatic pressure

$$P_{\mathrm{gr}} = \frac{\tau}{A} \frac{GM_{\mathrm{BH}}\dot{M}}{4\pi R^4} . \tag{8}$$

Here $A \leqslant 1$ is a dimensionless parameter which accounts for the flow geometry; τ is the time since the moment when accretion is stopped, and G is the gravitational constant. Combining these two relations one obtains the time required to restart accretion:

$$\tau = \frac{A}{2\pi^2 GM_{\mathrm{BH}}} \frac{\Psi^2}{\dot{M}} . \tag{9}$$

If there is no escape of the magnetic flux, i.e. the value of Ψ is increasing monotonically with time t, the interval between jet activations τ becomes longer with time, and asymptotically, given the quadratic dependence on Ψ in Eq.(9), the accretion process stops completely. Thus, the key condition for the quasi-periodic jet is the escape of the magnetic flux from a magnetically arrested region. We note that the escape of the magnetic field can be studied numerically only in the a 3D approach, i.e. a self-consistent description of this process remains out of the scope of this paper, and should be studied elsewhere. In what follows we adopt the critical value of Ψ_{cr}, when the flux escapes, as a free parameter. This parameter is in fact directly connected to the jet power through Eq.(6), thus the escape of the magnetic field defines not only the duration of the interval when the jet is paused, but also its available power during the jet ejection.

In the case of non-steady jet activity, the averaged jet luminosity is the key quantity characterizing the possible observational appearance of such jets. Obviously, the averaged power may depend on many different aspects of the involved processes, e.g. on the magnetic flux escape rate. In the simplest case, the critical magnetic flux value is smaller than the value required to pause the accretion: $\Psi_{\mathrm{cr}} < \Psi_0$, i.e. the magnetic flux starts to escape before the magnetic field can stop the accretion. Then, the jet is expected to be persistent with a power of

$$L_{\mathrm{BZ}} \approx 10^{35} \Psi_{\mathrm{cr},20}^2 \left(\frac{M_{BH}}{3M_\odot}\right)^{-2} \mathrm{erg\ s}^{-1}, \tag{10}$$

where $\Psi_{\mathrm{cr},20} = \Psi_{\mathrm{cr}}/10^{20}\mathrm{G\ cm}^2$. Given the assumed condition $\Psi_{\mathrm{cr}} < \Psi_0$, an upper limit for the jet luminosity can be obtained. Our numerical simulations show that the jet power $L_j = C\dot{M}c^2$, where $C \sim 0.05$, corresponds to the magnetic flux Ψ_0[1]. Here we note that, contrary to the widely accepted disk accretion paradigm, in the considered case the accretion rate cannot be estimated from the thermal radiation produced by the accreted matter.

In the case if the $\Psi_{\mathrm{cr}} > \Psi_0$, one should expect a more complicated temporary patterns in the system. Namely, the quasi-periodic behavior of the jet will not be vanished by the escape of the magnetic field, and the jet active phases will be separated by period of the jet silence of duration

$$\tau_{\mathrm{cr}} = \frac{A}{2\pi^2 GM_{\mathrm{BH}}} \frac{\Psi_{\mathrm{cr}}^2}{\dot{M}} . \tag{11}$$

Although the interval of the jet active phase depends on the process of the magnetic flux escape rate, the averaged jet luminosity can be estimated assuming that the escape process is rather slow as compared to the variability time. In this case, the duration of the active phase is roughly determined by time interval during which the accretion flow can keep the magnetic flux of Ψ_{cr} near the BH horizon. Accounting for the phases when the accretion stops, the matter ram pressure can be estimated as

$$P_{\mathrm{ram}} \approx \frac{\tau_{\mathrm{cr}} + t_{\mathrm{ac}}}{t_{\mathrm{ac}}} \frac{\dot{M}\sqrt{GM_{\mathrm{BH}}}}{4\pi R_{\mathrm{G}}^{5/2}}, \tag{12}$$

where t_{ac} is the duration of the jet active phase, and R_{G} is the gravitational radius of the BH. Using Eq.(7), one can obtain the following simple relation

$$\frac{t_{\mathrm{ac}}}{\tau_{\mathrm{cr}} + t_{\mathrm{ac}}} = \left(\frac{\Psi_0}{\Psi_{\mathrm{cr}}}\right)^2 . \tag{13}$$

---

[1] We note that the value of the parameter C depends on the BH rotation parameter a. Since the critical value of the magnetic flux Ψ_{cr} is a weak function of a (see e.g. Tchekhovskoy et al. 2011), the parameter C should be roughly proportional to the function $f(a)$ from Eq.(6). Thus, for a fast rotating BH, this parameter can have a value up to 10 times larger than the one obtained in our simulations.
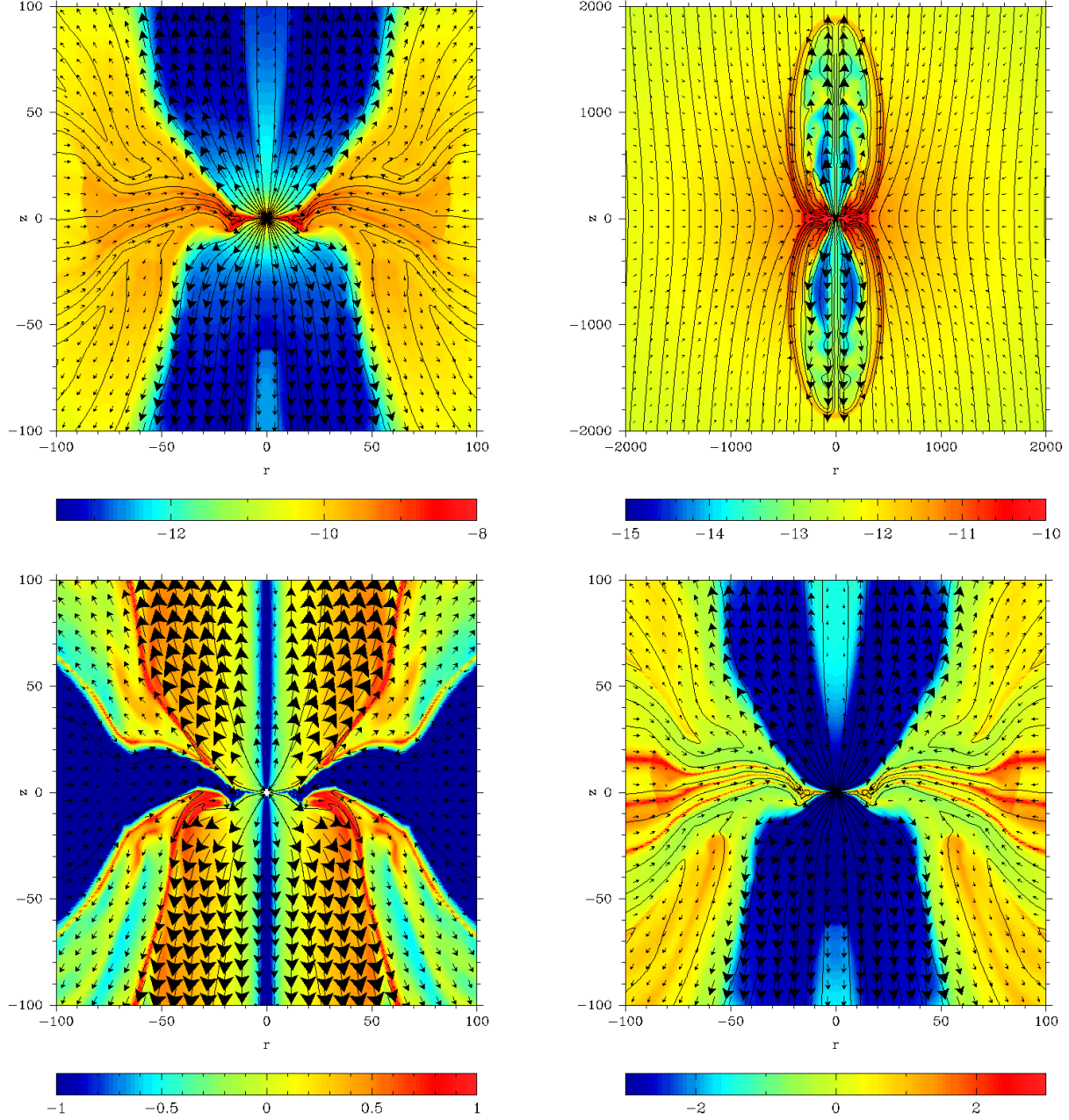
Figure 2. The magnetohydrodynamical properties of the flow: the solid lines show the magnetic field lines and arrows indicate the flow velocity (both the direction and the absolute value). The top panels show the distribution of the mass density ($\log \rho$ is shown by color) for the whole computation regions (top right panel), and for the zoomed central part (top left panel). The bottom panels indicate the ratio of the toroidal to poloidal magnetic field components ($\log B_\phi/B_p$ is shown by color in the bottom left panel); and the ratio of the gas to magnetic field pressures ($\log P_g/P_m$ is shown by color in the bottom right panel). The initial magnetic field in the stellar wind was assumed to be 10^3 G, and the accretion rate was selected to be $\dot{M}_{BH} = 8 \times 10^{-11} M_\odot \mathrm{yr}^{-1}$. The shown snapshot of the flow corresponds to the time moment $t = 0.145$ s after the accretion was initiated.

Since the BZ luminosity is proportional to Ψ^2, the jet averaged luminosity appears to be independent on the Ψ_{cr}:

$$< L_j >= \frac{t_{ac}}{\tau_{cr} + t_{ac}} \times L_{BZ}(\Psi_{cr}) = L_{BZ}(\Psi_0) \approx C\dot{M}c^2. \qquad (14)$$

Thus, for a broad range of parameters one can expect a universal dependence of the jet power on the accretion rate.

3.2   LS 5039 as a μQ

The universal averaged jet power expected in the suggested scenario allows to make meaningful estimates for the specific case of LS 5039 without 3D modeling. Indeed, the jet power depends on the accretion only and for the expected rate of $\dot{M} = 8 \times 10^{-11} M_\odot \mathrm{yr}^{-1}$ one obtains

$$L_{j,LS} \approx 3 \times 10^{35} \mathrm{erg\ s}^{-1}, \qquad (15)$$
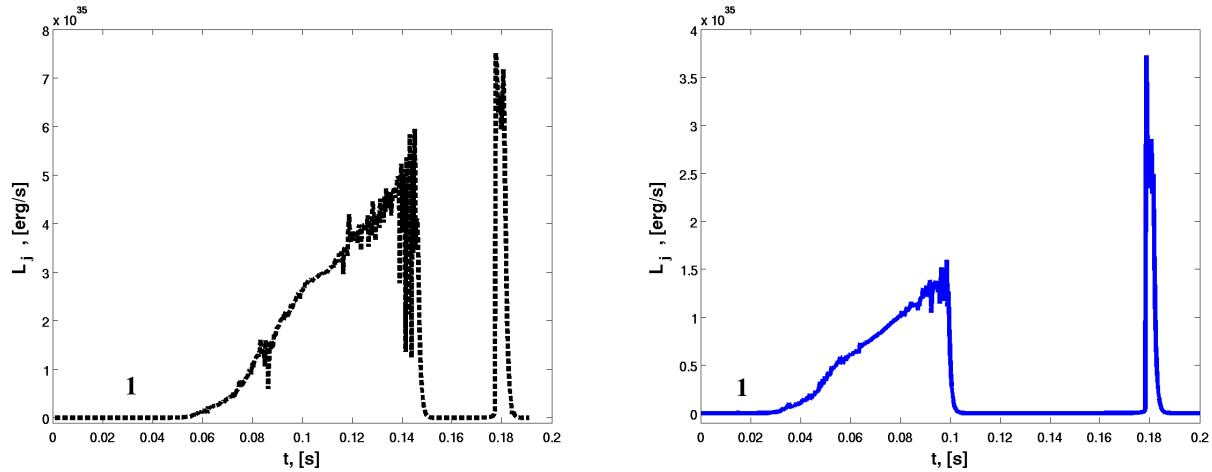
Figure 3. The jet luminosity as a function of time, *t*, since the moment when the accretion was started. The initial magnetic field in the stellar wind was assumed to be 10^3 G, and two accretion rates were considered $\dot{M}_{BH} = 8 \times 10^{-11} M_\odot \mathrm{yr}^{-1}$ (left panel); and $\dot{M}_{BH} = 1.5 \times 10^{-11} M_\odot \mathrm{yr}^{-1}$ (right panel).

per each jets. This estimate is similar to flux level detected in GeV energy band with *Fermi*/LAT telescope, thus to explain total non-thermal luminosity in the framework of the μQscenario one needs to invoke Doppler boosting of the emission. The Doppler boosting factor depends on the jet bulk Lorentz factor and the orientation of the jet in respect to the observer. The jet is orientated along the BH rotation axis, thus most likely it is directed perpendicularly to the orbital plane. The most feasible orbital inclination in LS 5039 is $i \sim 20° - 25°$ (Casares et al. 2005; Sarty et al. 2011), thus one can obtain an upper limit on the boosting factor: $\delta = 1/[\Gamma(1-\beta\cos i)] \approx 2\Gamma/(1 + \Gamma^2 i^2)$. If $\Gamma > 1/i$ the emission emitted toward Earth will be de-boosted, the optimal boosting can be achieved if $\Gamma \approx 1/i$. Thus, the largest Doppler boosting factor can be estimated as $\delta \lesssim 3$, which should lead to the apparent jet luminosity at the level of $< 10^{37} \mathrm{erg\,s}^{-1}$. For a relatively high, $> 10\%$ conversion rate of the jet luminosity to non-thermal emission, this energetics can explain the observed broad-band emission, although a dedicated modeling is required to shed the light on the possibility of the production of the detected radiation in the framework of the μQ scenario.

4 SUMMARY AND FINAL REMARKS

In this paper we study the wind accretion onto a rotating BH in close binary systems harboring a young massive star. It is shown that the angular momentum of the accreted stellar wind material is not sufficient for the formation of the accretion disk. On the other hand, the direct wind accretion can create conditions for the activation of the BZ process, and a powerful jet can be launched without any signatures of accretion, unlike it is usually seen in bright thermal X-ray binaries. The jet power is expected to be modulated on a sub-second scale, which can lead to an efficient jet loading with stellar wind material (see Derishev et al. 2011, in preparation). Although the flux escape mechanism should be properly treated with regard to the formation of persistent/quasi-periodic jets, a universal estimate on the jet averaged power is obtained. It is expected that approximately $\sim 10\%$ of the accreted rest energy can be chanelled into the jet. In the specific case of LS 5039, the obtained jet luminosity can be responsible for the observed non-thermal radiation if one invokes Doppler boosting, which can enhanced the apparent flux from the system and to be additional factor of the modula-

tion during the orbital motion. The future study of the non-thermal production in the framework of the suggested scenario, would require a self-consistent modelings of the wind accretion to the BH (Owocki et al. 2011), propagation of jet through binary system environment (Perucho & Bosch-Ramon 2008; Perucho et al. 2010), and non-thermal processes occurring in the jet.

REFERENCES

Abdo A. A., Ackermann M., Ajello M., Allafort A., Ballet J., Barbiellini G., Bastieri D., et al. 2011, ApJ, 736, L11+

Abdo A. A., Ackermann M., Ajello M., Atwood W. B., Axelsson M., Baldini L., Ballet J., et al. 2009a, ApJ, 701, L123

Abdo A. A., Ackermann M., Ajello M., Atwood W. B., Axelsson M., Baldini L., Ballet J., et al. 2009b, ApJ, 706, L56

Acciari V. A., Aliu E., Arlen T., Aune T., Beilicke M., Benbow W., Bradbury S. M., et al. 2011, ApJ, 738, 3

Acciari V. A., Aliu E., Arlen T., Bautista M., Beilicke M., Benbow W., Böttcher M., et al. 2009, ApJ, 700, 1034

Acciari V. A., Beilicke M., Blaylock G., Bradbury S. M., Buckley J. H., Bugaev V., Butt Y., et al. 2008, ApJ, 679, 1427

Aharonian F., Akhperjanian A. G., Anton G., Barres de Almeida U., Bazer-Bachi A. R., Becherini Y., Behera B., et al. 2009, A&A, 507, 389

Aharonian F., Akhperjanian A. G., Aye K.-M., Bazer-Bachi A. R., Beilicke M., Benbow W., Berge D., et al. 2005a, A&A, 442, 1

Aharonian F., Akhperjanian A. G., Aye K.-M., Bazer-Bachi A. R., Beilicke M., Benbow W., Berge D., et al. 2005b, Science, 309, 746

Aharonian F., Akhperjanian A. G., Bazer-Bachi A. R., Beilicke M., Benbow W., Berge D., Bernlöhr K., Boisson C., et al. 2006, A&A, 460, 743

Albert J., Aliu E., Anderhub H., Antonelli L. A., Antoranz P., Backes M., Baixeras C., et al. 2009, ApJ, 693, 303

Albert J., Aliu E., Anderhub H., Antoranz P., Armada A., Asensio M., Baixeras C., et al. 2006, Science, 312, 1771

Albert J., Aliu E., Anderhub H., Antoranz P., Armada A., Baixeras C., Barrio J. A., et al. 2007, ApJ, 665, L51

Artemova Y. V., Bisnovatyi-Kogan G. S., Igumenshchev I. V., Novikov I. D., 2006, ApJ, 637, 968

Bardeen J. M., Press W. H., Teukolsky S. A., 1972, ApJ, 178, 347

Barkov M. V., Komissarov S. S., 2008a, in F. A. Aharonian, W. Hofmann, & F. Rieger ed., American Institute of Physics Conference Series Vol. 1085 of American Institute of Physics Conference Series, Central engines of Gamma Ray Bursts. Magnetic mechanism in the collapsar model.. pp 608–611

Barkov M. V., Komissarov S. S., 2008b, MNRAS, 385, L28

Barkov M. V., Komissarov S. S., 2010, MNRAS, 401, 1644

Barkov M. V., Komissarov S. S., 2011, MNRAS, 415, 944

Bisnovatyi-Kogan G. S., Ruzmaikin A. A., 1974, Ap&SS, 28, 45

Bisnovatyi-Kogan G. S., Ruzmaikin A. A., 1976, Ap&SS, 42, 401

Blandford R. D., Begelman M. C., 1999, MNRAS, 303, L1

Blandford R. D., Znajek R. L., 1977, MNRAS, 179, 433

Bogovalov S., Khangulyan D., Koldoba A. V., Ustyugova G. V., Aharonian F. A., 2011, ArXiv e-prints

Bogovalov S. V., Khangulyan D. V., Koldoba A. V., Ustyugova G. V., Aharonian F. A., 2008, MNRAS, 387, 63

Bosch-Ramon V., Barkov M. V., 2011, ArXiv e-prints

Bosch-Ramon V., Khangulyan D., 2009, International Journal of Modern Physics D, 18, 347

Bosch-Ramon V., Khangulyan D., 2011, ArXiv e-prints

Bosch-Ramon V., Khangulyan D., Aharonian F. A., 2008, A&A, 482, 397

Casares J., 2007, in V. Karas & G. Matt ed., IAU Symposium Vol. 238 of IAU Symposium, Observational evidence for stellar-mass black holes. pp 3–12

Casares J., Ribó M., Ribas I., Paredes J. M., Martí J., Herrero A., 2005, MNRAS, 364, 899

Davies R. E., Pringle J. E., 1980, MNRAS, 191, 599

Dhawan V., Mioduszewski A., Rupen M., 2006, in VI Microquasar Workshop: Microquasars and Beyond LS I +61 303 is a Be-Pulsar binary, not a Microquasar

Dubus G., 2006, A&A, 456, 801

Dubus G., Cerutti B., Henri G., 2010, A&A, 516, A18+

Esin A. A., Narayan R., Cui W., Grove J. E., Zhang S.-N., 1998, ApJ, 505, 854

Igumenshchev I. V., 2008, ApJ, 677, 317

Illarionov A. F., Sunyaev R. A., 1975, åp, 39, 185

Ishii T., Matsuda T., Shima E., Livio M., Anzer U., Boerner G., 1993, ApJ, 404, 706

Johnston S., Manchester R. N., Lyne A. G., D'Amico N., Bailes M., Gaensler B. M., Nicastro L., 1996, MNRAS, 279, 1026

Kaisig M., Tajima T., Lovelace R. V. E., 1992, ApJ, 386, 83

Kennel C. F., Coroniti F. V., 1984, ApJ, 283, 710

Khangulyan D., Aharonian F. A., Bogovalov S. V., Ribo M., 2011, ArXiv e-prints

Khangulyan D., Hnatic S., Aharonian F., Bogovalov S., 2007, MNRAS, 380, 320

Khangulyan D. V., Aharonian F. A., Bogovalov S. V., Koldoba A. V., Ustyugova G. V., 2008, International Journal of Modern Physics D, 17, 1909

Kirk J. G., Ball L., Skjaeraasen O., 2000, in M. Kramer, N. Wex, & R. Wielebinski ed., IAU Colloq. 177: Pulsar Astronomy - 2000 and Beyond Vol. 202 of Astronomical Society of the Pacific Conference Series, Predictions of inverse Compton radiation from PSR B1259-63. pp 531–+

Kishishita T., Tanaka T., Uchiyama Y., Takahashi T., 2009, ApJ, 697, L1

Komissarov S. S., 1999, MNRAS, 303, 343

Komissarov S. S., 2004, MNRAS, 350, 427

Komissarov S. S., 2006, MNRAS, 368, 993

Komissarov S. S., Barkov M. V., 2007, MNRAS, 382, 1029

Komissarov S. S., Barkov M. V., 2009, MNRAS, 397, 1153

Kudritzki R., Puls J., 2000, ARA&A, 38, 613

Li J., Torres D. F., Zhang S., Chen Y., Hadasch D., Ray P. S., Kretschmar P., Rea N., Wang J., 2011, ApJ, 733, 89

Lovelace R. V. E., 1976, Nature, 262, 649

Moldón J., Johnston S., Ribó M., Paredes J. M., Deller A. T., 2011a, ApJ, 732, L10+

Moldón J., Ribó M., Paredes J. M., 2011b, A&A, 533, L7+

Narayan R., Igumenshchev I. V., Abramowicz M. A., 2003, PASJ, 55, L69

Narayan R., Yi I., 1994, ApJ, 428, L13

Negueruela I., Ribó M., Herrero A., Lorenzo J., Khangulyan D., Aharonian F. A., 2011, ApJ, 732, L11+

Owocki S. P., Okazaki A. T., Romero G., 2011, in C. Neiner, G. Wade, G. Meynet, & G. Peters ed., IAU Symposium Vol. 272 of IAU Symposium, Modeling TeV γ-rays from LS 5039: an active OB star at the extreme. pp 587–592

Perucho M., Bosch-Ramon V., 2008, A&A, 482, 917

Perucho M., Bosch-Ramon V., Khangulyan D., 2010, A&A, 512, L4+

Rea N., Torres D. F., Caliandro G. A., Hadasch D., van der Klis M., Jonker P. G., Méndez M., Sierpowska-Bartosik A., 2011, MNRAS, 416, 1514

Rea N., Torres D. F., van der Klis M., Jonker P. G., Méndez M., Sierpowska-Bartosik A., 2010, MNRAS, 405, 2206

Ribó M., Paredes J. M., Moldón J., Martí J., Massi M., 2008, A&A, 481, 17

Romanova M. M., Ustyugova G. V., Koldoba A. V., Lovelace R. V. E., 2009, MNRAS, 399, 1802

Ruffert M., 1997, åp, 317, 793

Ruffert M., 1999, åp, 346, 861

Ruffini R., Wilson J. R., 1975, Phys. Rev. D, 12, 2959

Sarty G. E., Szalai T., Kiss L. L., Matthews J. M., Wu K., Kuschnig R., Guenther D. B., Moffat A. F. J., Rucinski S. M., Sasselov D., Weiss W. W., Huziak R., Johnston H. M., Phillips A., Ashley M. C. B., 2011, MNRAS, 411, 1293

Takahashi T., Kishishita T., Uchiyama Y., Tanaka T., Yamaoka K., Khangulyan D., Aharonian F. A., Bosch-Ramon V., Hinton J. A., 2009, ApJ, 697, 592

Tam P. H. T., Huang R. H. H., Takata J., Hui C. Y., Kong A. K. H., Cheng K. S., 2011, ApJ, 736, L10+

Tchekhovskoy A., Narayan R., McKinney J. C., 2011, ArXiv e-prints

Uchiyama Y., Tanaka T., Takahashi T., Mori K., Nakazawa K., 2009, ApJ, 698, 911

Usov V. V., Melrose D. B., 1992, ApJ, 395, 575

Zabalza V., Bosch-Ramon V., Paredes J. M., 2011, ArXiv e-prints

Ziółkowski J., 2005, MNRAS, 358, 851